

# Magnetic properties and microstructures of FePt/Ti bilayer films sputter deposited onto glass amorphous substrates

H. Y. Sun,<sup>a)</sup> J. L. Xu, S. Z. Feng, Z. F. Su, and J. Hu  
*College of Physics Science and Information Engineering, Hebei Normal University,  
 Shijiazhuang 050016, China*

Y. P. Sun  
*Key Laboratory of Materials Physics, Institute of Solid State Physics, Chinese Academy of Sciences,  
 Hefei 230031, China*

(Received 19 September 2005; accepted 8 March 2006; published online 8 May 2006)

FePt/Ti granular films were fabricated onto glass amorphous substrates using a dc facing-target magnetron sputtering system at various Ti underlayer thickness, then annealed at temperature  $T_a$  ranging from 200 to 700 °C. In the FePt (30 nm)/Ti (1 nm) film annealed at 600 °C, the coercivity about 12 kOe is obtained. The results of x-ray diffraction indicate that a ternary FePtTi alloy is formed. Thus, the formation of the ternary FePtTi alloy is considered to play an important role in magnetic properties. © 2006 American Institute of Physics. [DOI: 10.1063/1.2195781]

Several  $L1_0$  structure alloys such as equiatomic FePt,<sup>1</sup> CoPt,<sup>2</sup> and FePd (Ref. 3) films are attractive candidates for ultrahigh density magnetic recording media because of the high magnetic anisotropy of  $L1_0$  phase. Among the  $L1_0$  alloys, Fe–Pt system has attracted much attention due to its high  $K_u$  value ( $\sim 7 \times 10^7$  erg/cm<sup>3</sup>), high coercivity, good corrosion resistance and large energy products  $(BH)_{\max}$ .<sup>1</sup> However, a high temperature treatment is necessary to transform phase from the disordered fcc structure to the  $L1_0$  structure. Recently, several attempts have been made to reduce the transition temperature, such as the introduction of underlayers<sup>4–6</sup> or seed layer,<sup>7–9</sup> the addition of third elements,<sup>10,11</sup> multilayering,<sup>12</sup> ion irradiation,<sup>13,14</sup> and *in situ* annealing.<sup>15</sup> Most of these investigations need single-crystal substrates and a complicated preparing process. For magnetic recording application, the applying of amorphous substrates and simple preparation conditions is more important. No attention has been paid to reduce the ordered temperature by applying the amorphous glass substrates and Ti underlayer. Kuo *et al.* have investigated (FePt)<sub>95</sub>Ti<sub>5</sub> films deposited onto natural-oxidized silicon wafer substrates, but the internal principle did not described explicitly.<sup>16</sup> It is very important to understand the relationship between concentration of Ti and the phase transition of FePt alloy.

In this letter, we propose a procedure for reducing the ordering temperature of the  $L1_0$  FePt-ordered alloy. The FePt/Ti bilayer films are deposited on glass amorphous substrate at room temperature. Because the atomic affinity between Fe and Pt is higher than that between Ti and Pt, we expect that the underlayer Ti atoms could move into the ordered FePt layer when the samples are annealed. Crystal structure, magnetic properties, and microstructure of the films will also be presented.

FePt (30 nm)/Ti( $t$  nm) bilayer films,  $t=0, 1, 3, 5,$  and  $6$ , were deposited directly on glass substrates using dc facing-target magnetron sputtering system at room temperature. The base pressure was better than  $1.5 \times 10^{-5}$  Pa. High-purity argon of 0.5 Pa was flown during sputtering. A mosaic target consisting of high purity iron disk (99.99%) overlaid with

high purity platinum pieces (99.99%) was used. After the deposition, the samples were annealed in vacuum. The annealing temperature was varied from 200 to 700 °C, and the annealing time was fixed at 30 min. The crystallographic structures of the samples were analyzed by x-ray diffraction (XRD) with  $\text{CuK}\alpha$  radiation. The magnetic properties of these films were measured with vibrating sample magnetometer and physical property measurement system at room temperature, respectively. The atomic ratio of the FePt (30 nm)/Ti (1 nm) was 99:1 by means of energy disperse x-ray diffractometer. The atomic force microscopy (AFM) images and magnetic force microscopy (MFM) images were scanned using scanning probe microscope.

Because the lattice parameters of fcc phase and  $L1_0$  phase are very close, the XRD patterns are also similar except that there are several addition peaks for  $L1_0$  phase due to reduced lattice symmetry. To find out the appropriate underlayer thickness of Ti to obtain the most appropriate ordered structure, a different thickness of Ti layer were characterized. Figure 1 shows the XRD patterns for FePt (30 nm)/Ti( $t$  nm) films,  $t=0, 1, 5,$  and  $6$ , annealed at 600 °C for 30 min. It can be seen that the monolayer FePt film shows fct (111) orientation peak. At  $t=1$  nm, the (111) peak becomes weaker, and strong (001), (110), (002), and (200) superlattice peaks of the fct ordered FePt can be observed. This result is confirmed by the maximum of  $H_c$  as

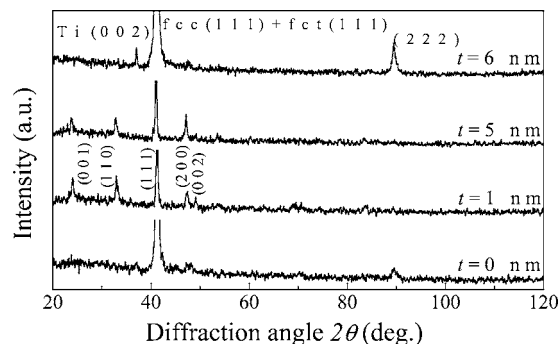


FIG. 1. XRD patterns of various FePt/Ti films at different Ti layer thickness.

<sup>a)</sup>Electronic mail: hysun@165e.com

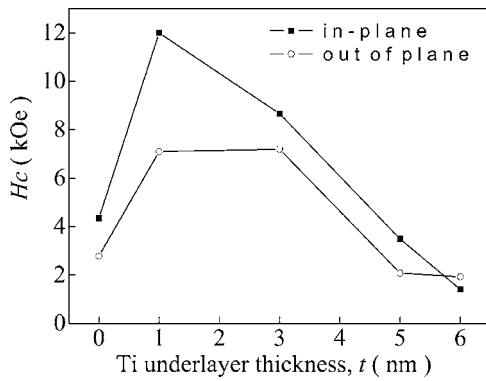


FIG. 2. Coercivity  $H_c$  of FePt/Ti films as a function of the Ti underlayer thickness  $t$  after annealing at 600 °C.

shown in Fig. 2. When the thickness of Ti layer is further increased up to 5 nm, (001), (110) peaks become weak, (002) peak vanishes and (111) peak becomes stronger. At  $t = 6$  nm, fct (111), (222) and fcc (111) peaks become stronger, and Ti (002) peak appears. The results reveal that the FePt particles begin to form an ordered  $L1_0$  phase when  $t$  is within 5 nm. We think this may be attributed to that the thin Ti layers separate island-like grain distributing on the substrates. Once Ti grains between FePt particles are developed, high diffusion barriers prohibit further grain growth and coalescence. Thus, the isolation of Ti atoms plays an important role in inducing the ordered texture. However, thicker Ti layer was no longer separate but rather continuous, so inter-diffusion between the underlayer and magnetic film becomes easy. Therefore, Ti atoms can diffuse into the  $L1_0$  textured magnetic grains, which result in the frustration of ordered phase. This result is confirmed by analyses of alloy phase diagrams, which can reveal that excess Ti atoms will form alloy with Fe and Pt atoms easily. Therefore, the thickness of Ti underlayer plays a crucial role in determining the magnetic properties and the surface morphology.

Figure 2 shows the coercivities ( $H_c$ ) of the FePt/Ti bilayer films as a function of Ti underlayer thickness ( $t$ ) after annealing at 600 °C for 30 min.  $H_c$  has a strong dependence on Ti thickness. Huge coercivity of 12 kOe, which is measured parallel to the film plane, is obtained for  $t=1$  nm. The out of plane coercivity up to 8.5 kOe is obtained in the film with  $t=3$  nm.

XRD patterns of various FePt (30 nm)/Ti (1 nm) double layer films at different annealed temperatures ( $T_a$ ) are shown in Fig. 3. It can be seen that high annealing temperature gives almost (111) texture and low annealing temperature leads to the development of other peaks. The sample annealed at 300 °C shows (001), (110), (111), (200), (202), and (311) superlattice of the fct ordered FePt. These reveal that the ordered  $L1_0$  ordering phase of FePt have begun to be formed at  $T_a=300$  °C. With  $T_a$  increasing, the characteristic peaks of  $L1_0$  chemical ordering increase. At  $T_a=600$  °C, (001), (110), and (111) peaks become the strongest and sharpest. Further annealed at 700 °C, result changes largely. The intensity of the (111) peaks increases sharply, reflecting strong FePt(111) texturing. The results reveal that the FePt particles begin to form an ordered  $L1_0$  phase when  $T_a$  is within 600 °C. This result is confirmed by the maximum of  $H_c$  as shown in Fig. 4.

Magnetic measurements reveal that there is a strong  $T_a$  dependence of the magnetic properties. Figure 4 shows the

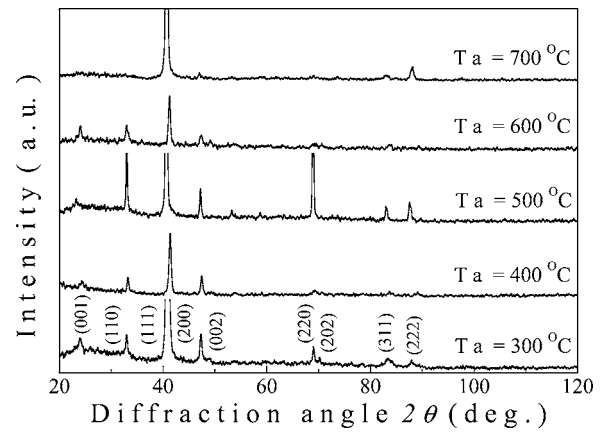


FIG. 3. XRD patterns of various FePt (30 nm)/Ti (1 nm) bilayer films at different annealed temperatures ( $T_a$ ).

magnetic properties of the FePt (30 nm)/Ti (1 nm) bilayer samples as a function of the annealing temperature ( $T_a$ ). Large  $H_c$  of about 7.1 kOe, which is measured perpendicular to the film plane, is obtained for  $T_a=500$  and 600 °C at room temperature. Meanwhile, the maximum value of the in-plane  $H_c$  is obtained about 12 kOe for  $T_a=600$  °C. With decreasing the  $T_a$ , the two directions  $H_c$  both decreases dramatically, but still keeps a value of about 3 and 4.1 kOe for  $T_a=400$  °C. The squareness ( $S=M_r/M_s$ ) of the films first increases with the increase of  $T_a$  and reaches the maximum at 600 °C. Further increasing  $T_a$  causes  $S$  to decrease. The  $M_s$  of the films increases slightly for perpendicular direction with increasing the  $T_a$  within  $T_a=300$  °C. However, it decreases slightly for parallel direction. Beyond 300 °C, the  $M_s$  increases drastically and then decreases with further increasing the  $T_a$ . The maximum value of the out of plane  $M_s$  and the in-plane  $M_s$  is obtained at  $T_a=400$  °C and  $T_a=500$  °C, respectively. The increase in magnetization with increasing annealing temperature is mainly due to the increase of fcc phase. With further increasing annealing temperature, magnetization decreases may be attributed by the increase of the fct phase content, because the  $M_s$  value of the fct phase is lower than that of the fcc phase.

Figure 5 shows the AFM (left) and MFM (right) images of FePt (30 nm)/Ti (1 nm) with different  $T_a$ . All AFM and MFM images are obtained in the same region of film in a

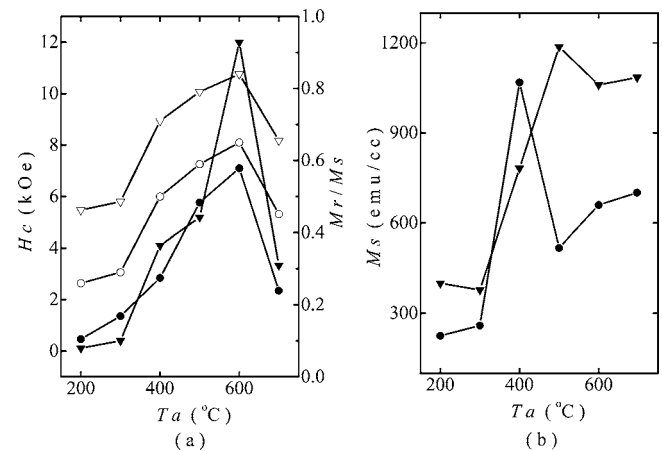


FIG. 4. (a) The coercivities (filled marks) and squareness (open marks), (b) the saturation magnetization ( $M_s$ ), respectively, measured ( $\blacktriangledown$ ) parallel to the film plane and ( $\bullet$ ) perpendicular to the plane as a function of the  $T_a$ .

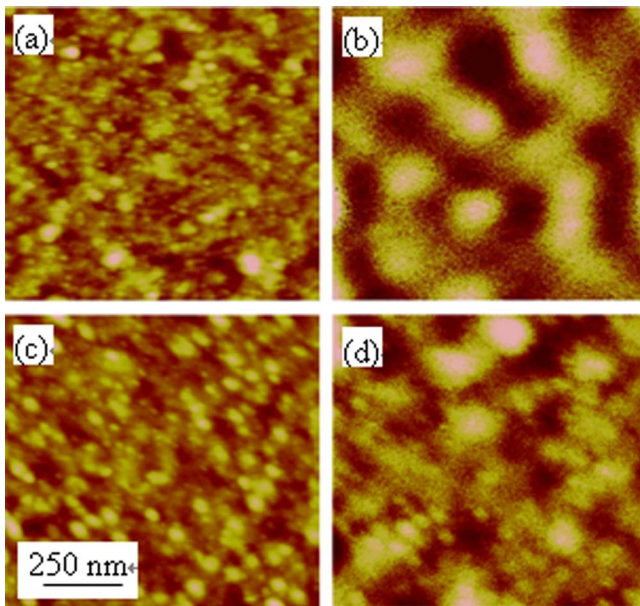


FIG. 5. (Color online) AFM (left) and MFM (right) images of FePt(30 nm)/Ti(1 nm) with different  $T_a$ . (a) and (b)  $T_a=500$  °C, (c) and (d)  $T_a=600$  °C.

consecutive scan. AFM observation indicates that the films are composed of island-like particles at  $T_a=500$  °C, and of separated island-like patches at  $T_a=600$  °C. This suggests that the island-like particles grew gradually as  $T_a$  increases, and became separated island-like patches. The average roughness  $R_a$  of the sample annealed at 500 °C is 0.695 nm, and of the sample annealed at 600 °C is 0.515 nm. The MFM images give the domain structures of the particles in the films. The MFM measurement detects the magnetic force gradient arising from magnetic charge on the surface. It may be noticed that the domains look continuous across the adjacent particles/patches, and the average size of the magnetic domains decreases dramatically by annealing at 600 °C. Smaller magnetic domains size is preferred for the high density recording media.

In conclusion, the FePt (30 nm)/Ti (1 nm) bilayer film which annealed at 600 °C for 30 min in vacuum exhibits high in-plane coercivity of 12 kOe, and out of plane coercivity of 7.1 kOe. In addition, the out of plane coercivity up to 8.5 kOe was obtained in FePt (30 nm)/Ti (3 nm) annealed at 600 °C for 30 min. The average roughness  $R_a$  of the FePt (30 nm)/Ti (1 nm) is 0.515 nm. X-ray diffraction analyses revealed the formation of FePtTi alloy. The FePtTi alloy annealed at 300 °C begin to form an ordered  $L1_0$  phase, which reveals that it is a promising candidate for high-density magnetic recording media application.

This work is supported by the National Natural Science Foundation of China (Grant No. 10274018), the Foundation of Hebei Provincial Education Department (Grant No. 2002116), and the Key Foundation of Hebei Normal University (Grant No. Z200102).

- <sup>1</sup>B. Zhang and W. A. Soffa, IEEE Trans. Magn. **MAG-26**, 1388 (1990).
- <sup>2</sup>M. Yu, Y. Liu, and D. J. Sellmyer, J. Appl. Phys. **87**, 6959 (2000).
- <sup>3</sup>K. Sato and Y. Hirotsu, J. Appl. Phys. **93**, 6291 (2003).
- <sup>4</sup>Y. Zhang, J. Wan, V. Skumryev, S. Stoyanov, Y. Huang, and G. C. Hadjipanayis, Appl. Phys. Lett. **85**, 5343 (2004).
- <sup>5</sup>Y. Shimada, T. Sakurai, T. Miyazaki, O. Kitakami, and S. Okamoto, J. Magn. Magn. Mater. **262**, 329 (2003).
- <sup>6</sup>C. H. Lai, C. C. Chiang, and C. H. Yang, J. Appl. Phys. **97**, 10H310 (2005).
- <sup>7</sup>T. Seki, T. Shima, K. Takanashi, Y. Takahashi, and E. Matsubara, Appl. Phys. Lett. **82**, 2461 (2003).
- <sup>8</sup>M. L. Yan, Y. F. Xu, X. Z. Li, and D. J. Sellmyer, J. Appl. Phys. **97**, 10H309 (2005).
- <sup>9</sup>J. Wan, Y. Huang, Y. Zhang, M. J. Bonder, G. C. Hadjipanayis, and D. Weller, J. Appl. Phys. **97**, 10J121 (2005).
- <sup>10</sup>H. Kura and T. Sato, J. Appl. Phys. **96**, 5771 (2004).
- <sup>11</sup>T. Maeda, T. Kai, A. Kikisu, T. Nagase, and J. Akiyama, Appl. Phys. Lett. **80**, 2147 (2002).
- <sup>12</sup>C. P. Luo and D. J. Sellmyer, Appl. Phys. Lett. **75**, 3162 (1999).
- <sup>13</sup>D. Ravelosona, C. Chappert, V. Mathet, and H. Bernas, J. Appl. Phys. **87**, 5771 (2000).
- <sup>14</sup>C. H. Lai, C. H. Yang, and C. C. Chiang, Appl. Phys. Lett. **83**, 4550 (2003).
- <sup>15</sup>Y. K. Takahashi, M. Ohnuma, and K. Hono, Jpn. J. Appl. Phys., Part 2 **40**, L1367 (2002).
- <sup>16</sup>C. M. Kuo, P. C. Kuo, W. C. Hsu, C. T. Li, and A. C. Sun, J. Magn. Magn. Mater. **209**, 100 (2000).